

Time-resolved light scattering by photoexcited V_2O_3

Nardeep Kumar, Armando Rúa, Ramón Díaz, Iván Castillo, Brian Ayala, Sandra Cita, Félix Fernández and Sergiy Lysenko
Department of Physics, University of Puerto Rico, Mayaguez, Puerto Rico 00681, USA

ABSTRACT

Using ultrafast angle-resolved light scattering technique, we were able to trigger photoinduced phase transition processes in V_2O_3 film grown on a glass substrate. The phase transition is caused by photoacoustic wave in the film and appears as coherent oscillations of scattering signal at various time scales. These processes strongly depend on the size of microstructures constituting the V_2O_3 film. One of the key findings of our study is the presence of a size dependent phase transition threshold for V_2O_3 microstructures, where small size structures ($\lesssim 0.5\mu\text{m}$) have lowest contribution to the phase transition. The presence of this threshold can be well described by considering uneven internal strain in the films which is one of the key parameters controlling phase transition dynamics in various vanadium oxides.

INTRODUCTION

Vanadium sesquioxide (V_2O_3) has metallic characteristics at room temperature with a corundum crystal structure (space group $R3c$) [1], it is considered as a Mott-Hubbard material in which electron-electron correlations play a crucial role [2-4]. Since its discovery in 1946 by Foëx [5, 6], it has been a focus of various experimental as well as theoretical studies. One of the qualities of V_2O_3 is related to its temperature–doping phase diagram [7] which shows three phases: a paramagnetic metal (PM) phase, antiferromagnetic insulator phase (AI), and paramagnetic insulator (PI) phase. V_2O_3 shows a metal-insulator phase transition (MIT) from a paramagnetic metal (PM) phase to a low-temperature antiferromagnetic insulator (AI) phase around ~ 150 K. This phase transition is followed by a lattice distortion from a corundum lattice to monoclinic lattice symmetry. Along with thermal parameters, photons can also alter the electronic properties of various oxides, and trigger their phase transition (PT) [8]. The light-induced PT dynamics of V_2O_3 is a complex process which depends upon sample temperature, initial phase state and photoinduced strain [9]. Photexcitation is a powerful approach to investigate potential pathways for phase transitions.

In this paper, we report the observation of transient nonlinear optical (NLO) response of V_2O_3 films at room temperature (~ 293 K) by using ultrafast optical diffraction technique. By using angle-resolved light scattering technique combined with femtosecond pump-probe spectroscopy, we statistically investigate transient processes in V_2O_3 films and obtain information about correlations between photoexcited transition dynamics and film morphology.

EXPERIMENTAL DETAILS

Sample preparation

The V_2O_3 thin films were deposited on glass (SiO_2) substrates by reactive DC magnetron sputtering from a vanadium (99.95% purity) target. The distance between the 2" diameter target and the substrates was 10 cm and substrates were kept at $550^\circ C$ during growth. Background pressure was $\sim 10^{-5}$ Torr and sputtering pressure was 20 mTorr, with argon and oxygen flows of 35.0 and 1.4 standard cubic centimeters per second, respectively. Sputtering power was 200 W. With this process a sample of thickness 370 nm was prepared. Figure 1c shows surface topography of the V_2O_3 sample. The average grain size value is ~ 90 nm. X-ray diffraction studies (figure 1d) of synthesized samples showed pure stoichiometric V_2O_3 corundum phase at room temperature. To find the absorption coefficient of the sample we measured transmittance for 800 nm. By making use of transmittance and Beer Lambert's law, we obtained an absorption coefficient (α) of 0.0237 nm^{-1} , which gives a penetration depth d ($d=1/\alpha$) of 42 nm.

Time-resolved elastic light scattering spectroscopy

The experimental setup to investigate light-induced metal to insulator phase transition dynamics of V_2O_3 is schematically shown in figure 1a. Ultrashort pulses with ~ 130 fs duration and central wavelength $\lambda=800$ nm, which act as a pump pulse in our experiment, were produced at 1kHz repetition rate by the regenerative amplifier of a Spectra-Physics femtosecond laser system. A Beta Barium Borate (BBO) nonlinear crystal is used to generate $\lambda = 400$ nm second harmonic, which acts as probe pulse. Circularly polarized pump and vertically polarized probe beams were focused to a spot size of 0.6 mm and $70 \mu\text{m}$ respectively. Both pump and probe

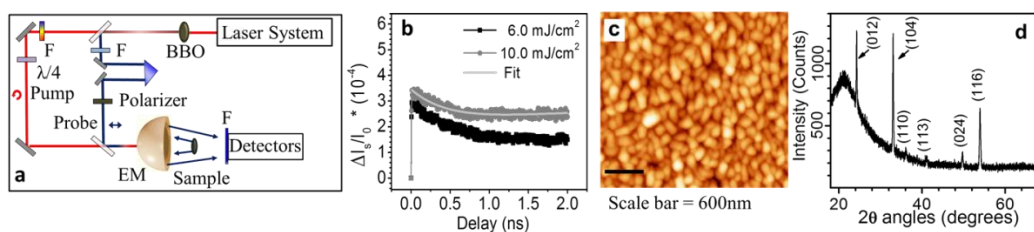


Figure 1. Panel (a) shows the experimental system. Panel (b) shows transient differential scattering signal (I_s) integrated over hemisphere and normalized to the incident intensity (I_0). The light gray curves show exponential fits for scattering curves for fluence 6 mJ/cm^2 and 10 mJ/cm^2 . Panel (c) shows surface topography of V_2O_3 thin films sample observed by atomic force microscope. Panel (d) shows XRD pattern of V_2O_3 sample.

pulses were incident normal to the sample surface. An elliptical mirror (EM) was used to collect and focus the light scattered by the sample surface to photodiode and charge couple device (CCD) detectors. Color filters, denoted by F in figure 1a, were used to block the pump beam from reaching the detectors and to filter out the second harmonic of the pump pulse.

DISCUSSION

Light scattering response of photoexcited V_2O_3

Light scattering is a powerful technique which can be used to detect small structural variations on the surface of thin films and hence allows studying structural heterogeneity of materials. The change in the film inhomogeneity and optical properties upon PT contributes significantly to the intensity of the scattered light. The observed scattering by V_2O_3 is a combination of light scattering due to dielectric constant variation, structural irregularities, and their cross-correlation effects [10, 11]. The pump-probe femtosecond scattering technique was used to monitor the MIT dynamics in a V_2O_3 film of thickness 370 nm on SiO_2 substrate. Figure 1b shows the evolution of the diffraction signal on a 2 ns time scale, for pump fluence of 6 mJ/cm^2 (black curve) and 10 mJ/cm^2 (dark gray curve). Ultrafast excitation of V_2O_3 initiates, after an instantaneous increase of scattering within $\sim 500 \text{ fs}$, a nearly exponential decay process lasting several nanoseconds. The curves obtained at 6 mJ/cm^2 and 10 mJ/cm^2 optical excitations of the sample were fitted by double exponential functions (figure 1b). From the fits we see there are two relaxation processes. The first process has decay time on the order of $\sim 600 \text{ ps}$ while the second process decays more slowly ($>2 \text{ ns}$).

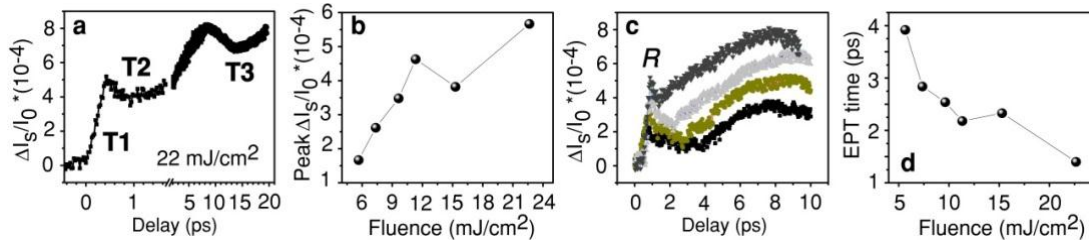


Figure 2. Panel (a) shows differential scattering signal versus probe delay for fluence 22 mJ/cm^2 . Panel (b) shows the peak intensity of the scattering signal within 1 ps as a function of the pump fluence. Panel (c) shows evolution of differential scattering signal within 10 ps for 6 mJ/cm^2 (dark gray curve), 7 mJ/cm^2 (light gray curve), 15 mJ/cm^2 (gray curve), and 22 mJ/cm^2 (black curve) pump fluence. Panel (d) summarizes the characteristic times of electron-phonon thermalization (EPT) process with pump fluence.

Figure 2a shows the light-induced transient change in V_2O_3 scattering versus pump-probe delay within 20 ps at fluence of 22 mJ/cm^2 . Due to the photoexcitation of nonequilibrium transient state and nonuniform distribution of metallic and insulator phases, we see an increase of light scattering within the first few picoseconds. From these measurements the transient nonlinear optical (NLO) response of V_2O_3 can be divided into three main processes: (i) an ultrafast generation within 1ps, of a long-lasting photoexcited state, marked as T1, (ii) a relaxation process within the few picosecond time scale, denoted by T2, and (iii) transient processes T3 visible within 20 picoseconds. The initial process T1 is assigned to excitation of transient electronic states. The density of these states and the intensity of scattered light (figure 2b) increase with pump fluence. The process T2 corresponds to electron-phonon thermalization and strongly depends on the level of optical excitation. The characteristic time of this process was defined as a time between the peak point "R" in the figure 2c and the point where scattering signal starts to increase (starting point of the process T3). It is interesting to note that this time is inversely proportional to the fluence, as shown in figure 2d. Therefore, this time can be attributed to the transfer of sufficient energy to trigger the process T3, where at higher optical excitation the time to initiate the process T3 is less. The process T3 is assigned to the coherent acoustic phonon process accompanied by photoacoustical strain-induced PM-PI phase transition [9]. As

can be seen from figure 2c, the starting point of this process is affected by the rate of electron-phonon thermalization. Thus, electron-phonon thermalization is an intermediate step between initially generated photoexcited electronic state T1 and the process T3. The recovery process starts after several hundred picoseconds and completes in several hundred nanoseconds (not shown here), after damping of acoustical phonons and heat transfer to the substrate. Figure 1b shows a relaxation process within ~600 ps which can be assigned to thermalization of acoustical phonons and, possibly, of coupled electron-phonon states. In order to resolve the size-dependent optical dynamics of V_2O_3 , we performed angular measurements of light scattering within the hemisphere in front of the sample.

Ultrafast angle-resolved elastic light scattering

Angle-resolved elastic light scattering is a very powerful technique to study the statistical properties of the surface [12, 13]. The scattering signal measured within the hemisphere, is represented by the Bidirectional-Scatter-Distribution-Function, defined elsewhere [14], which is a function of polar angle θ and azimuthal angle ϕ . The angular distribution of scattered light, mapped by the BSDF indicatrix, provides information about ultrafast PT dynamics not only for the overall films surface but also for individual structures with different azimuthal orientations and spatial frequencies.

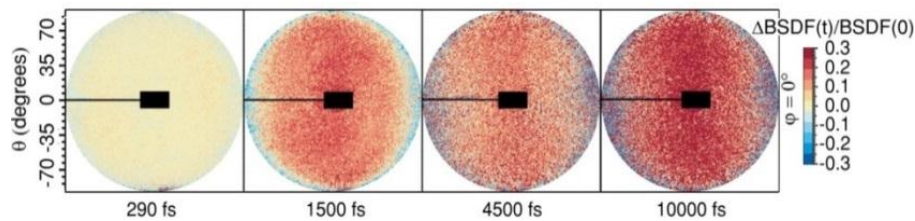


Figure 3. Ultrafast $\Delta\text{BSDF}(t)/\text{BSDF}(0)$ diffraction patterns of photoexcited V_2O_3 surface as a function of pump-probe pulse delay. A black rectangle at the center of indicatrices shows the position of sample holder.

By mapping the scattering data as a relative change $\Delta\text{BSDF}(t)/\text{BSDF}(0)$, where $\Delta\text{BSDF}(t) = \text{BSDF}(t) - \text{BSDF}(0)$, additional information about V_2O_3 PT dynamics can be explored. The relative change of the scattering pattern, for 290 fs, 1500 fs, 4500 fs, and 10000 fs, is shown in figure 3b. The rapid change of light scattering between 300 fs and 1500 fs shows that the initial NLO processes occur within 1 ps. Moreover, angular dependence of $\Delta\text{BSDF}(t)/\text{BSDF}(0)$ indicates that the size of V_2O_3 grains significantly affects transient NLO dynamics in the film. To investigate the V_2O_3 phase transition dynamics with respect to characteristic size of film structural irregularities, we map the cross sections of scattering patterns (figure 4a) from the V_2O_3 sample for different spatial frequencies (at azimuthal angle $\phi=220^\circ$) with respect to probe delay. There are four prominent oscillations visible for the microstructures up to $\sim 2 \mu\text{m}^{-1}$ spatial frequency. These prominent oscillations are visible at 8-12 ps, 22-35 ps, 45-57 ps, and 63-80 ps marked in figure 4a by 1, 2, 3 and 4 white lines respectively. These oscillations can be assigned to PM-PI phase transition process induced by coherent acoustic phonons [9]. The signal rise between 8-12 ps corresponds to the increase of scattering signal, as was observed in figure 2a.

The next noticeable increase of scattering signals at 22-35 ps, 45-57 ps, and 63-80 ps also can be assigned to PM-PI phase transition induced by coherent acoustic phonons. The period of these oscillations is ~ 27 ps. This could be due to the fact that optical pulse excites V_2O_3 within, approximately, penetration depth (~ 42 nm) which is several times less than the overall thickness of the film. These prominent oscillations were not resolved in the differential scattering scans. This is another advantage of angle-resolved elastic light scattering technique, which helps to easily resolve hidden features of NLO dynamics. Corresponding curves of BSDF versus spatial frequency f are shown in figure 4b for 0 and 80 fs. Although all curves show irregular BSDF (f) maxima, the BSDF (f) profile and positions of all diffraction peaks in the scattering indicatrix remain the same. This implies that the surface geometry of V_2O_3 films on glass substrates also remains the same.

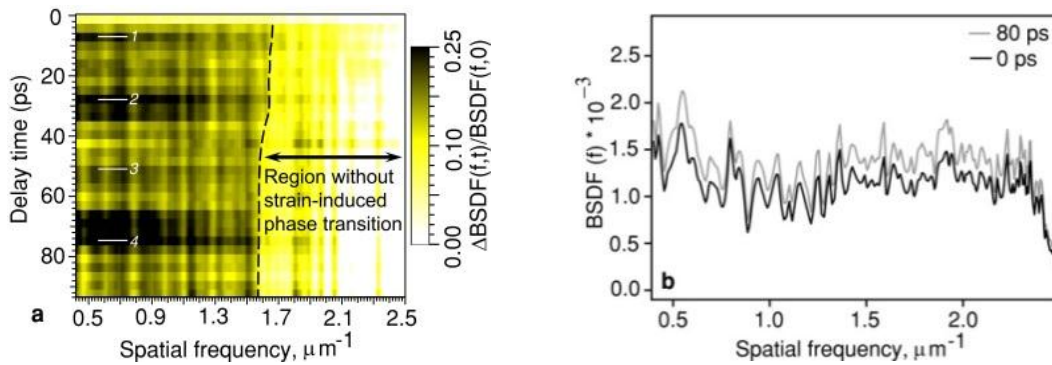


Figure 4. Panel (a) shows evolution of normalized scattering intensity for different spatial frequencies for 100 ps temporal range. White lines and numbers represent four prominent oscillations visible in the signal. Panel (b) shows the cross-section of BSDF with respect to different spatial frequencies for probe delay of 0 ps and 80 ps.

From the map of scattering cross-section, we clearly see a variation of scattering intensity, and hence V_2O_3 PT, with respect to different spatial frequencies. The map shows that above $f \sim 2 \mu\text{m}^{-1}$, the transient optical nonlinearity is less prominent than for lower spatial frequencies. There is a sharp drop in the scattering intensity above $f \cong 2 \mu\text{m}^{-1}$. Since spatial frequency f and characteristic size d of irregularities are related as $f = 1/d = \sin \theta / \lambda$, the spatial frequency of $2 \mu\text{m}^{-1}$ corresponds to $0.5 \mu\text{m}$ characteristic sized microstructures of the V_2O_3 film. The sharp drop in the scattering intensity for smaller structures ($\lesssim 0.5 \mu\text{m}$) indicates the existence of a size-dependent threshold for strain-induced PM-PI transition in photoexcited V_2O_3 . This fact has not previously been observed in V_2O_3 , and is an important finding. Since the PM-PI transition is directly related to photoinduced strain in V_2O_3 , one possible cause of the observed threshold for smaller grains is associated with a presence of uneven internal strain in the film. In this case the induced strain in smaller structures with sizes less than $\sim 0.5 \mu\text{m}$ is significantly lower as compared to larger structures. This implies that in V_2O_3 films the PM-PI phase transition does not take place uniformly over the entire photoexcited areas of the film. Moreover, as shown previously for VO_2 films, even a small change in the internal strain of the film could result in the formation of new domain patterns and hence affects the scattering intensity [15]. While the photoinduced PT dynamics of V_2O_3 is different from that in VO_2 , our results also show strong dependence of V_2O_3 MIT on structure size and suggest that the strain is one of the key parameters controlling PM-to-PI phase transition in V_2O_3 .

CONCLUSIONS

In summary, femtosecond angle-resolved light scattering spectroscopy provides a unique opportunity to investigate photoexcited dynamics of V_2O_3 . Ultrafast optical excitation results in instantaneous change of V_2O_3 optical properties within ~ 500 fs. However, optical response associated with paramagnetic metal to paramagnetic insulator phase transition induced by photoacoustical strain was observed on picosecond time scale. The evolution of scattering signal reveals coherent oscillations of material optical properties. With this approach, we were able to resolve these oscillations up to 70 ps. The scattering experiments herein demonstrate a key feature of V_2O_3 MIT at room temperature in which nonlinear optical dynamics significantly depends upon the size of film microstructures. Our results show that larger structures ($\gtrsim 0.5 \mu\text{m}$) show a major contribution whereas smaller structures have negligible or no contribution to V_2O_3 transient nonlinear processes induced by photoacoustical strain. Our analysis shows that the use of angle-resolved light scattering opens a possible new route to study V_2O_3 MIT.

ACKNOWLEDGMENTS

The authors are pleased to acknowledge the support for this work by the U.S. Army Research Office under Award No. W911NF-15-1-0448, and by the College of Arts and Sciences of the University of Puerto Rico at Mayagüez.

REFERENCES

1. D. B. McWhan and T. M. Rice, *Phys. Rev. Lett.* **22**, 887 (1969).
2. D. B. McWhan, T. M. Rice, and J. P. Remeika, *Phys. Rev. Lett.* **23**, 1384 (1969).
3. N. F. Mott, *Rev. Mod. Phys.* **40**, 677 (1968).
4. C. Castellani, C. R. Natoli, and J. Ranninger, *Phys. Rev. B* **18**, 5001 (1978).
5. M. Foëx, *C. R. Acad. Sci. (Paris)* **223**, 1126 (1946).
6. M. Foëx, S. Goldsztaub, R. Wey, J. Jaffray, R. Lyand, and J. Wucher, *J. Rech. Cent. Nat. Rech. Sci. Lab. Bellevue (Paris)* **21**, 237 (1952).
7. D. B. McWhan and J. P. Remeika, *Phys. Rev. B* **2**, 3734–3750 (1970).
8. E. Abreu, S. Wang, J. G. Ramírez, M. Liu, J. Zhang, K. Geng, I. K. Schuller, and R. D. Averitt, *Phys. Rev. B* **92**, 085130 (2015).
9. M. K. Liu, B. Pardo, J. Zhang, M. M. Qazilbash, Sun Jin Yun, Z. Fei, Jun-Hwan Shin, Hyun-Tak Kim, D. N. Basov, and R. D. Averitt, *Phys. Rev. Lett.* **107**, 066403 (2011).
10. J. M. Elson, *Phys. Rev. B* **30**, 5460 (1984).
11. J. M. Elson, *Waves Random Media* **7**, 303 (1997).
12. M. Zerrad, M. Lequime, and C. Amra, *Appl. Opt.* **53**, A297–A304 (2014).
13. J. C. Stover, *Optical Scattering: Measurements and Analysis*, 3rd ed. (SPIE Optical Engineering, 1995).
14. J. C. Stover, *Optical Scattering Measurement and Analysis*. (McGraw-Hill, 1990).
15. S. Lysenko, F. Fernández, A. Rúa, J. Aparicio, N. Sepúlveda, J. Figueroa, K. Vargas, and J. Cordero, *J. Appl. Phys.* **117**, 184304 (2015).